DOI:10.11835/j.issn.2096-6717.2020.128　　开放科学(资源服务)标识码(OSID):

Study on the shear bearing capacity of RC shear walls using artificial neural networks

GUO Wenye, *ZHANG Jianxin*

(School of Civil and Transportation Engineering; Civil Engineering Technology Research Center of Hebei Province, Hebei University of Technology, Tianjin 300401, P. R. China)

Abstract: In various areas of civil engineering, the artificial neural network (ANN) model is used to solve complex problems. In this study, ANN models were used to predict the shear bearing capacity of RC shear walls. Based on the results of 160 experiments, a database was constructed that included the performance of RC shear walls under cyclic loading. One hundred and forty samples were chosen to train the ANN models, and 20 were used for validation. There were fourteen inputs parameters: concrete compressive strength, aspect ratio, axial compression ratio, vertical bar yield strength, horizontal bar yield strength, web vertical reinforcement ratio, web horizontal reinforcement ratio, boundary region vertical reinforcement ratio, boundary region horizontal reinforcement ratio, sectional area ratio, sectional height thickness ratio, total section area, wall height, and section shape. ANN1 and ANN2 were normalized in intervals of [0, 1] and [0.1, 0.9], respectively. The shear force of the RC shear walls was the output data for both models. The predictions by the ANN models and the code methods from GB 50011 and ACI 318 were compared. The results reveal that the developed models exhibit better prediction and generalization capacity for RC shear walls than the code methods.

Keywords: artificial neural network; shear wall; reinforced concrete; model prediction; shear bearing capacity

基于神经网络的钢筋混凝土剪力墙抗剪承载力研究

郭文烨,张健新

(河北工业大学 土木与交通学院;河北省土木工程技术研究中心,天津 300401)

摘　要:神经网络(ANN)模型作为土木工程领域中一种有效的方法能够用于解决复杂的问题。基于试验数据采用神经网络对钢筋混凝土剪力墙的抗剪承载力进行预测,收集 160 个钢筋混凝土剪力墙在低周往复荷载下的试验数据,建立数据库,选取 140 个试验样本对 ANN 模型进行训练,20 个试验样本进行测试验证。ANN1 和 ANN2 有 14 个输入参数:混凝土抗压强度、剪跨比、轴压比、竖向钢筋强度、横向钢筋强度、墙体竖向分布钢筋配筋率、墙体水平分布钢筋配筋率、边缘构件纵向钢筋配筋率、边缘构件横向钢筋配筋率、边缘构件与截面面积比、截面高厚比、总截面面积、墙高和截面形状,输入数据分别被归一化到区间[0, 1]和[0.1, 0.9]。两个模型的输出数据均为剪力。对比分析 ANN 模型预测的钢筋混凝土剪力墙抗剪承载力与采用规范 GB 50011 和 ACI 318-14 公式

Received: 2020-05-29

Foundation items: Natural Science Foundation of Hebei Province (No. E2018202290)

Author brief: GUO Wenye (1997-), main research interest: reinforced concrete structure, E-mail: elena_999@163.com.
ZHANG Jianxin (corresponding author), PhD, E-mail: zhangjianxin505@126.com.

计算的抗剪承载力，结果表明，神经网络模型能够精确地预测钢筋混凝土剪力墙的抗剪承载力，具有较好的预测和泛化能力。

关键词：神经网络；剪力墙；钢筋混凝土；模型预测；抗剪承载力

中图分类号：TU398.2 **文献标志码**：A **文章编号**：2096-6717(2021)01-0137-08

1 Introduction

Reinforced concrete (RC) shear walls are often used in building structures due to their capacity to resist lateral loads under seismic action[1]. The concrete strength, aspect ratio, axial compression ratio, vertical or horizontal web reinforcement ratio, and vertical or horizontal boundary region reinforcement ratio are critical design parameters that govern the lateral load resistance capacity of RC shear walls[2-3]. The formula used in domestic and foreign codes to calculate the shear bearing capacity is an empirical formula determined by statistical analysis, that reflects the main physical and geometric parameters and considers the factors that influence the reliability. Differences in the calculation model and calculation method are incorporated in current codes, such as GB 50011, ACI 318, and EC2. Furthermore, the strength of the concrete used in the formula for calculating the shear bearing capacity is also different. Generally, most existing methods of calculating the shear bearing capacity of RC shear walls are based on models with limited experimental data, such as shear walls using high-strength steel bars. Therefore, further research on more reliable and effcient structural assessement is needed.

ANNs have been used for simulating engineering problems[4-6]. To predict the axial bearing capacity, Du et al.[7] suggested two ANN models of rectangular concrete-filled steel tubular columns. Kotsovou et al.[8] established an ANN model to predict the load bearing capacity of beam-column joints. However, the ANN models and experimental data are limited. In this study, shear bearing capacity predictions of RC shear walls were developed using artificial neural networks. The developed ANN model provides a reference for prefabricated concrete shear walls, the seismic performance of which are equivalent to cast-in-place RC walls[9-12].

2 Data collection

As shown in Fig. 1, test results for 160 RC shear walls with rectangular or barbell sections was found in the literature [2-3, 13-29]. The test information included all parameters that may have an impact on the behavior of the RC shear walls. The test samples exhibited good deformation ability. The parameters for all samples were consistent.

The size parameters of the wall (b, h, and H), the yield strength of the horizontal reinforcements f_y, the concrete compressive strength f_c, the aspect ratio λ, the axial compression ratio μ, and the shear force V are included to train and test the ANN models. Finally, 160 test samples were obtained and are summarized in Table 1.

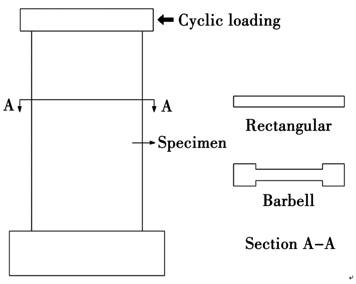

Fig. 1 Typical test setup under cyclic loading and section for RC shear walls

3 Artificial neural networks

3.1 Background information

ANN is an operational model that mimics the neural network of the human brain from the perspective of information processing. ANN is an artificial intelligence technology that can solve complex problems based on input parameters. The

Table 1 Test data of RC shear walls

Number	b/mm	h/mm	H/mm	f_y/MPa	f_c/MPa	λ	μ	Source
11	102-152	1 905	4 572	429-464	21.8-51.8	2.4	0-0.134	Oesterle et al.[13]
20	70	750	825	470	23.8-42.3	1.1-2.1	0-0.171	Lefas et al.[14]
6	60	600	1 200	540	31.8-45.8	2	0	Pilakoutas et al.[15]
11	100	1 200	1 200-1 800	585	21.6-27.5	1-1.5	0-0.07	Salonikios et al.[16]
10	150	1 200-1 300	2 500	422-540	28-40	1.9-2.1	0-0.083	Riva et al.[17]
26	80-120	1 000-1 700	525-1 000	314-471	15.7-24.2	0.4-1	0	Hidalgo et al.[18]
6	150	2 000	4 520-4 560	547-601	38.3-45.6	2.3	0.05-0.13	Dazio et al.[19]
8	76	1 016	2 540	420-448	38.9-130.8	2.5	0.03-0.09	Liu et al.[20]
5	152	1 219	1 829-2 438	472-477	47.1-57.5	1.5-2	0.02-0.08	Tran et al.[21]
3	100	700	1 750	469	27.4	2.5	0.15-0.35	Alarcon et al.[22]
6	75-100	700	1 330-1 750	446-469	27.4	1.9-2.5	0.15	Hube et al.[23]
6	51	254	1 067	552	30.3-36.5	4.2	0	Wang et al.[24]
8	200	1 500	1750	617-653	46.1-70.3	1.2	0.07	Park et al.[2]
5	203	2 032	2 032	450-770	38-44	1	0	Min et al.[3]
7	100	1 000	1 200-2 200	630	93.5-110.7	1.1-1.2	0.05	Teng et al.[25]
4	100	1 000	2 350	341-640	41.6	2.25	0.3	Guo et al.[26]
9	85-100	1 600	1 750	446-632	28.9	1.1	0	Hube et al.[27]
5	100	1 200	1 000-1 600	479-638	38.7-53.9	1-1.5	0.13-0.2	Chen et al.[28]
4	200	1 000	2 000	472-641	34.9	2	0.1	Liu et al.[29]

effects of these parameters are not explicitly illustrated or quantified. ANNs have the ability to learn, summarize, classify, and predict, and it have been achieved remarkable results in many practical applications over the past years. In this study, ANNs are used to predict the shear bearing capacity of RC shear walls.

This study uses a back-propagation (BP) algorithm, as shown in Fig. 2. A typical artificial neuron is shown in Fig. 3. Three layers are included in the ANNs: input layer, hidden layer, and output layer. Each layer comprises k neurons, three neurons, and two neurons, respectively.

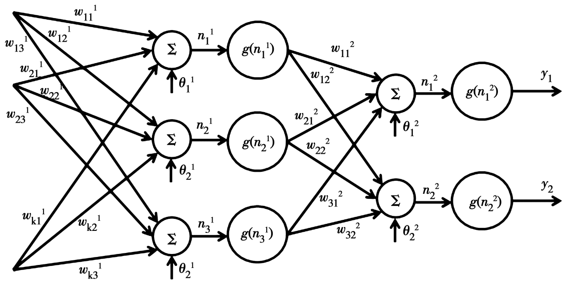

Fig. 2 A typical ANN

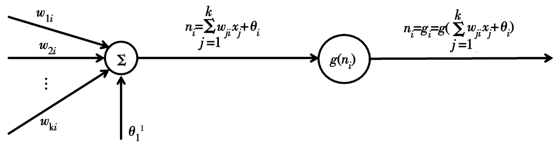

Fig. 3 A typical artificial neuron

The connections between interrelated neurons with a set specific weight are multiplied by the input data produced by the neuron. The values obtained in a particular layer are passed through the link and summed up with the bias (refer to Fig. 2)[8]. A predefined activation is used to represent the relationship between the inputs and the outputs, as shown in the following

$$y_i = g(v) = g(\sum_{j=1}^{k} w_{ij}x_j + \theta_i) \tag{1}$$

where y_i is the output of the ANN, w_{ij} is the weight coefficients of the j^{th} neuron, x_j is the input data, θ_i is the bias of the neuron, and $g(\cdot)$ is the activation function. In this study, input and hidden layers used sigmoid activation functions, and the output layer used the tan-sigmoid activation function.

3.2 Input and output data

The input parameters were selected based on the dominant effect of the parameters on the behavior of the RC shear wall, and included the concrete compressive strength (f_c), the aspect ratio (λ), the axial compression ratio (μ), the vertical reinforcement yield strength ($f_{y,vw}$), the horizontal reinforcement yield strength ($f_{h,vw}$), the vertical reinforcement web ratio (ρ_{vw}), the horizontal reinforcement web ratio (ρ_{hw}), the vertical reinforcement boundary region ratio (ρ_{vc}), the horizontal reinforcement boundary region ratio (ρ_{hc}), the sectional area ratio of the boundary region to the total cross-section area (A_b/A_g), the sectional height thickness ratio (l_w/t_w), the total section area (A_g), the wall height (H), and the section shape (the rectangular section is "0" and the barbell section is "1").

Since the performance of the RC shear walls specified in the code is determined by the limit of the shear load capacity, we take the maximum shear (V_{max}) as the target parameter. The maximum and minimum values of the input and output data are listed in Table 2. Table 3 shows the correlation between the input parameters used for the prediction of the shear bearing capacity of the RC shear walls. Some parameters are weakly correlated while others are strongly correlated. For example, the correlation coefficient between the l_w/t_w and A_b/A_g was -0.763, which indicates a strong negative relationship. The correlation coefficient between the H and λ was 0.449, which indicates a weak positive relationship. The sequence of the correlation for the input parameters from strong to weak were A_g, ρ_{vc}, ρ_{hc}, f_c, A_b/A_g, section shape, $f_{y,vw}$, $f_{h,vw}$, H, ρ_{hw}, λ, ρ_{vw}, μ, and l_w/t_w.

Table 2 Maximum and minimum values of the input and output data

Parameters/targets	Min. value	Max. value	Units
f_c	15.7	130.8	MPa
λ	0.4	4.2	
μ	0	0.35	
$f_{y,vw}$	314	770	MPa
$f_{h,vw}$	314	806	MPa
ρ_{vw}	0	0.025	
ρ_{hw}	0	0.024 5	
ρ_{vc}	0	0.097	
ρ_{hc}	0	0.062 4	
A_b/A_g	0.188	0.77	
l_w/t_w	4.98	21.25	
A_g	19 355	412 902	mm^2
H	525	4 572	mm
Section	0	1	
V_{max}	15.35	2 579	kN

Table 3 Correlation matrix for input parameters

Parameters/targets	f_c	λ	μ	$f_{y,vw}$	$f_{h,vw}$	ρ_{vw}	ρ_{hw}	ρ_{vc}	ρ_{hc}	A_b/A_g	l_w/t_w	A_g	H	Section shape
f_c	1.000	0.249	0.090	0.312	0.249	0.135	0.463	0.576	0.489	0.603	−0.374	0.270	0.268	0.570
λ	0.249	1.000	0.006	0.312	0.284	0.279	0.354	0.227	0.016	0.547	−0.731	−0.124	0.449	0.487
μ	0.090	0.006	1.000	0.017	−0.031	−0.055	−0.019	0.179	−0.054	0.092	−0.085	0.045	0.038	−0.101
$f_{y,vw}$	0.312	0.312	0.017	1.000	0.611	0.155	0.159	0.432	0.422	0.318	−0.482	0.156	0.158	0.187
$f_{h,vw}$	0.249	0.284	−0.031	0.611	1.000	0.129	0.068	0.301	0.359	0.211	−0.300	0.115	0.151	0.121
ρ_{vw}	0.135	0.279	−0.055	0.155	0.129	1.000	0.602	0.281	0.116	0.255	−0.274	−0.383	−0.099	−0.002
ρ_{hw}	0.463	0.354	−0.019	0.159	0.068	0.602	1.000	0.387	0.289	0.571	−0.475	0.018	0.245	0.402
ρ_{vc}	0.576	0.227	0.179	0.432	0.301	0.281	0.387	1.000	0.450	0.514	−0.505	0.306	0.183	0.333
ρ_{hc}	0.489	0.016	−0.054	0.422	0.359	0.116	0.289	0.450	1.000	0.308	−0.219	0.367	0.204	0.397
A_b/A_g	0.603	0.547	0.092	0.318	0.211	0.255	0.571	0.514	0.308	1.000	−0.763	0.135	0.339	0.492
l_w/t_w	−0.374	−0.731	−0.085	−0.482	−0.300	−0.274	−0.475	−0.505	−0.219	−0.763	1.000	−0.104	−0.344	−0.468
A_g	0.270	−0.124	0.045	0.156	0.115	−0.383	0.018	0.306	0.367	0.135	−0.104	1.000	0.662	0.197
H	0.268	0.449	0.038	0.158	0.151	−0.099	0.245	0.183	0.204	0.339	−0.344	0.662	1.000	0.367
Section shape	0.570	0.487	−0.101	0.187	0.121	−0.002	0.402	0.333	0.397	0.492	−0.468	0.197	0.367	1.000

To minimize the deviation of the ANN and low convergence rates, the values of the input and output data are normalized using Eq. (2).

$$x_i{}' = \frac{x_i - x_{\min}}{x_{\max} - x_{\min}}, \text{for } i = 1, 2, \ldots, n. \quad (2)$$

3.3 Training and testing of the ANNs

In this study, the network was built using the ANN toolbox in MATLAB. The BP network with 15 hidden layers was used to build the model of RC shear walls. The 160 experimental samples were randomly divided into two groups, 140 samples for training, and 20 samples for testing. In order to verify the effect of normalization equation on the ANNs prediction, the two control groups ANN1 and ANN2 were normalized in the range [0, 1] and [0.1, 0.9].

The training process of the neural network involves adjusting the network's weights and deviations (initially randomly assigned) to optimize the network's performance in the iterative process. The error performance index of the forward network is MSE, which is the mean square error between the network output and the target. The neural network would modify the network node weight, according to MSE. At the same time, in order to reduce the error in each iteration, ANN used the back-error propagation algorithm. After the error was calculated, the weights and bias were readjusted.

The calibration procedure of the ANN model is shown in Fig. 4. This was repeated until one of the following conditions was met: 1) After 500 training sessions, the algorithm will stop the training process. 2) The error-index reaches 10^{-5}. 3) The validation check occurs 10 times.

The ANN values (ANN-output) and test values (targets) are illustrated in Fig. 5. The ANNs predicted values were close to the experimental values with good deformation ability, indicating that the ANN1 and ANN2 models successfully learned the relationship between input and output data. In addition, the predicted values and test values that were closer to each other in different normalized ranges were in the range [0, 1] rather than the range [0.1, 0.9].

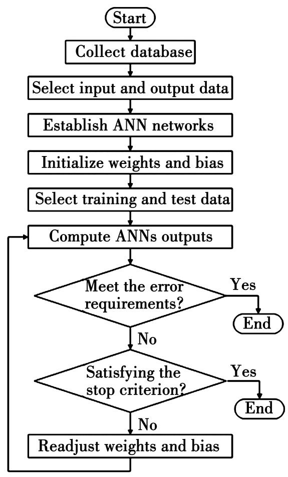

Fig. 4 Calibration procedure of the ANN model

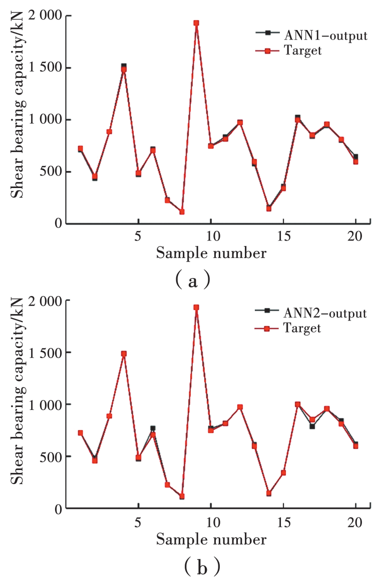

Fig. 5 ANN predicted values and test values

The ratio of output to target OTR, mean value *MV*, and standard deviation *SD* are used to evaluate the behavior of the model.

$$\mathrm{OTR}_i = O_i / T_i \quad (3)$$

$$MV = \frac{1}{n} \sum_{i=1}^{n} \frac{O_i}{T_i} \quad (4)$$

$$SD = \sqrt{\frac{1}{n} \sum_{i=1}^{n} (1 - \mathrm{OTR}_i)^2} \quad (5)$$

Where O_i and T_i are the prediction values of the ANN models and the maximum shear of the experimental samples, respectively. n is the total sample number.

Curves of OTR and sample number for ANN1, ANN2, GB 50011, and ACI 318 are presented in Fig. 6. Two predicted values in the ANN1 model exhibited the errors of 8.1% and 8.7%, which were overestimated. Two predicted values in the ANN2 model exceeded the error of 8.0%. One was underestimated and the other was overestimated. The *SD* was 0.036 1 in ANN1 and 0.041 2 in ANN2 (refer to Table 4). Therefore, the ANN1 model was superior to the ANN2 model in calculating the shear bearing capacity of RC shear walls.

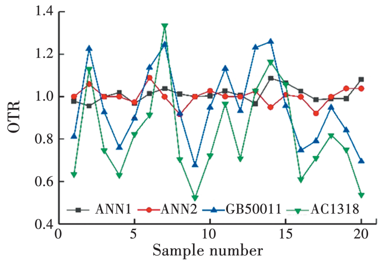

Fig. 6 OTRs-sample numbers curves for ANN1, ANN2, GB 50011, and ACI 318

Table 4 *MVs* and *SDs* with testing data

Variables	ANN1	ANN2	GB 50011	ACI 318
MV	1.010 9	1.002 2	0.954 4	0.825 6
SD	0.036 1	0.041 2	0.189 7	0.223 6

4 Comparative studies of ANN models and design codes

The methods proposed by GB 50011 and ACI 318 are presented as follows

$$V_u = \frac{1}{\lambda - 0.5}(0.4 f_t b h_0 + 0.13 N \frac{A_w}{A}) + f_{yv}\frac{A_{sh}}{s} h_0 \tag{6}$$

$$V_u = \varphi(V_c + V_s) \tag{7}$$

$$V_c = \min\left\{0.27\sqrt{f'_c}hd + \frac{N_u d}{4 l_w}, \left[0.05\sqrt{f'_c} + \frac{l_w\left(0.1\sqrt{f'_c} + 0.2\frac{N_u}{l_w h}\right)}{\frac{M_u}{V_u} - \frac{l_w}{2}}\right]hd\right\} \tag{8}$$

$$V_s = \frac{A_v f_y d}{s_2} \tag{9}$$

The outputs of the RC shear walls are the results calculated by the formulas Eqs. (6) to (9).

Fig. 6 shows the OTRs calculated by ANN1, ANN2, GB 50011, and ACI 318. Table 4 lists *MVs* and *SDs* using the testing data for ANN1, ANN2, GB 50011, and ACI 318.

Results predicted by the ANN1 and ANN2 models matched those calculated by GB 50011 and ACI 318 very well.

The results predicted by the ANN1 and ANN2 models matched those calculated by GB 50011 and ACI 318 very well. There were two outputs with an error of over 8% for both ANN1 and ANN2, but they did not exceed 10%. Two out of twenty in ANN1 were overestimated. One was overestimated in ANN2, and the other was underestimated. These results show that the ANN model exhibited a significant improvement compared to the standard GB 50011 and ACI 318. Compared with the experimental data, fourteen results predicted by GB 50011 exceed 10% difference based on the *OTRs*. There were sixteen predicted results with errors exceeding 10% in ACI 318. The *SDs* of ANN1 and ANN2 were 0.036 1 and 0.041 2, much lower than those of GB 50011 and ACI 318 (refer to Table 3). Compared with GB 50011 and ACI 318, the ANNs exhibited better performance on predicting the shear bearing capacity of RC shear walls.

There were thirteen results with errors exceeding 10% in GB 50011 and three in ACI 318 were underestimated. The *MVs* of the results predicted by GB 50011 and ACI 318 were 0.954 4 and 0.825 6, respectively. ANN models exhibited higher *MVs* than GB 50011 and ACI 318, indicating that the formulas were conservative in GB 50011 and ACI 318 due to the usage of high strength materials. The *SD* of GB 50011 and ACI 318 reached 0.189 7 and 0.223 6, which were larger than the ANN models.

The ANN1 and ANN2 models had the two largest *MVs*, while ANN1 and ANN2 exhibited smaller *SDs*. Thus, ANN models can accurately predict the shear bearing capacity of RC shear walls. Compared with the design codes, ANN models may be safer.

5 Conclusions

Two ANN models with fourteen input parameters were developed, based on experimental data. An efficient learning model based on ANNs was proposed to evaluate the load bearing capacity of RC shear walls. The prediction results show that ANN models predict the load bearing capacity favorably using parameters such as the aspect ratio, the axial compression ratio, the concrete and reinforcement strength, the boundary region and web reinforcement ratio, and the sectional ratio and size, thus accurate predictions can be provided.

The ANN1 and ANN2 models exhibit a better correlation with the experimental results than the codes GB 50011 and ACI 318. The ANN models exhibit better accuracy in prediction and generalization capacity. The BP algorithm can be effectively adopted in the shear strength prediction of RC shear walls.

Application of developed ANNs can be extended by further experimental tests including other shaped sections as input data. More studies on RC shear walls including high strength concrete and high strength reinforcements are valuable for the structures adopting RC shear walls.

Acknowledgements

The authors would like to acknowledge the financial support from the Natural Science Foundation of Hebei Province (No. E2018202290).

References:

[1] NI X Y, CAO S Y, LIANG S, et al. High-strength bar reinforced concrete walls: Cyclic loading test and strength prediction [J]. Engineering Structures, 2019, 198: 109508.

[2] PARK H G, BAEK J W, LEE J H, et al. Cyclic loading tests for shear strength of low-rise reinforced concrete walls with grade 550 MPa bars [J]. ACI Structural Journal, 2015, 112(3): 299-310.

[3] CHENG M Y, HUNG S C, LEQUESNE R D, et al. Earthquake-resistant squat walls reinforced with high-strength steel [J]. ACI Structural Journal, 2016, 113(5): 1065-1076.

[4] SIAM A, EZZELDIN M, EL-DAKHAKHNI W. Machine learning algorithms for structural performance classifications and predictions: Application to reinforced masonry shear walls [J]. Structures, 2019, 22: 252-265.

[5] TRUNG N T, SHAHGOLI A F, ZANDI Y, et al. Moment-rotation prediction of precast beam-to-column connections using extreme learning machine [J]. Structural Engineering and Mechanics, 2019, 70(5): 639-647.

[6] GEYER P, SINGARAVEL S. Component-based machine learning for performance prediction in building design [J]. Applied Energy, 2018, 228: 1439-1453.

[7] DU Y S, CHEN Z H, ZHANG C Q, et al. Research on axial bearing capacity of rectangular concrete-filled steel tubular columns based on artificial neural networks [J]. Frontiers of Computer Science, 2017, 11(5): 863-873.

[8] KOTSOVOU G M, COTSOVOS D M, LAGAROS N D. Assessment of RC exterior beam-column joints based on artificial neural networks and other methods [J]. Engineering Structures, 2017, 144: 1-18.

[9] SOUDKI K, WEST J S, RIZKALLA S H, et al. Horizontal connections for precast concrete shear wall panels under cyclic shear loading [J]. PCI Journal, 1996, 41(3): 64-80.

[10] SMITH B J, KURAMA Y C, MCGINNIS M J. Behavior of precast concrete shear walls for seismic regions: comparison of hybrid and emulative specimens [J]. Journal of Structural Engineering, 2013, 139(11): 1917-1927.

[11] CHEN Y, ZHANG Q, FENG J, et al. Experimental study on shear resistance of precast RC shear walls with novel bundled connections [J]. Journal of Earthquake and Tsunami, 2019, 13: 1940002.

[12] LI J B, WANG L, LU Z, et al. Experimental study of L-shaped precast RC shear walls with middle cast-in-situ joint [J]. The Structural Design of Tall and Special Buildings, 2018, 27(6): e1457.

[13] OESTERLE R G, FIORATO A E, JOHAL L S, et al.

Earthquake resistant structural walls tests of isolated walls [R]//Report to National Science Foundation, Skokie (IL, USA): PCA Construction Technology Laboratories, 1976.

[14] LEFAS I D, KOTSOVOS M D, AMBRASEYS N N. Behavior of reinforced concrete structural walls: strength, deformation characteristics, and failure mechanism [J]. ACI Structural Journal, 1990, 87(1): 23-31.

[15] PILAKOUTAS K, ELNASHAI A. Cyclic behavior of RC cantilever walls, part I: Experimental results [J]. ACI Structural Journal, 1995, 92(3): 271-281.

[16] SALONIKIOS T N, KAPPOS A J, TEGOS I A, et al. Cyclic load behavior of low-slenderness reinforced concrete walls: Design basis and test results [J]. ACI Structural Journal, 1999, 96(4): 649-660.

[17] RIVA P, FRANCHI A. Behavior of reinforced concrete walls with welded wire mesh subjected to cyclic loading [J]. ACI Structural Journal, 2001, 98(3): 324-334.

[18] HIDALGO P, LEDEZMA C, JORDAN R. Seismic behavior of squat reinforced concrete shear walls [J]. Earthquake Spectra, 2002, 18(2): 287-308.

[19] DAZIO A, BEYER K, BACHMANN H. Quasi-static cyclic tests and plastic hinge analysis of RC structural walls [J]. Engineering Structures, 2009, 31(7): 1556-1571.

[20] LIU X, BURGUEÑO R, EGLESTON E, et al. Inelastic web crushing performance limits of high-strength-concrete structural wall: Single wall test program: Report No. CEE-RR-2009/03 [R]. Michigan State University, East Lansing, MI, 2009, 281.

[21] TRAN T. Experimental and analytical studies of moderate aspect ratio reinforced concrete structural walls [D]. University of California, 2012.

[22] ALARCON C, HUBE M A, DE LA LLERA J C. Effect of axial loads in the seismic behavior of reinforced concrete walls with unconfined wall boundaries [J]. Engineering Structures, 2014, 73: 13-23.

[23] HUBE M A, MARIHUÉN A, DE LA LLERA J C, et al. Seismic behavior of slender reinforced concrete walls [J]. Engineering Structures, 2014, 80: 377-388.

[24] WANG Y. Effects of web reinforcement discontinuities on the seismic response of structural walls [D]. West Lafayette, Indiana: Purdue University. 2014.

[25] TENG S, CHANDRA J. Cyclic shear behavior of high-strength concrete structural walls [J]. ACI Structural Journal, 2016, 113(6): 1335-1345.

[26] GUO R, ZHU K. Experimental research on seismic behavior of RC shear wall with 600 megapascal high-strength reinforced bars [J]. Industrial Construction, 2017, 47(6): 34-39.

[27] HUBE M, SANTA-MARIA H, LOPEZ M. Experimental campaign of thin reinforced concrete shear walls for low-rise constructions [C]// Proceedings of Sixteenth World Conference on Earthquake, Santiago, 2017.

[28] CHEN X L. Study on seismic performance of RC shear wall structure reinforced with HRB600 high strength reinforcement [D]. Chongqing: Chongqing University, 2018.

[29] LIU Y. Experimental study on seismic performance of concrete shear walls with 600 MPa steel bars [D]. Nanjing: Southeast University, 2019.

(编辑 章润红)